Filter Property of InAs and Mgo Polar Semiconductor in Dielectric Medium of Different Radii

Abstract

Owing to its excellent electrical, mechanical, thermal and optical properties, graphene has attracted great interests since it was successfully exfoliated in 2004. Its two dimensional nature and superior properties meet the need of surface plasmons and greatly enrich the field of plasmonics. Recent progress and applications of graphene plasmonics will be reviewed, including the theoretical mechanisms, experimental observations, and meaningful applications. With relatively low loss, high confinement, flexible feature, and good tunability, graphene can be a promising plasmonic material alternative to the noble metals. Optics transformation, plasmonic metamaterials, light harvesting etc. are realized in graphene based devices, which are useful for applications in electronics, optics, energy storage, THz technology and so on. Moreover, the fine biocompatibility of graphene makes it a very well candidate for applications in biotechnology and medical science. Here is a study taking InAs and MgO polar semiconductor is being done with keeping it in dielectric medium again having different radii.

Daya Shankar
Assistant Professor,
Deptt.of Physics,
University of Lucknow,
Lucknow, U.P.

Abhishek Tiwari
Associate Professor
Deptt.of Physics,
(Applied Sciences)
SRIMT, DR APJ Abdul Kalam
Technical University,
Lucknow, U.P.

Keywords: Graphene, Plasmonics, Light harvesting, Filters.

Introduction

The author investigated the spherical surface properties Filter property of InAs and MgO polar semiconductor in dielectric medium of different radiiwith BlochHydrodynamical Model by deriving spatial dispersion relation for Surface Plasmons, Phonons and Polariton.Defferent dielectric medium can also be used for deferent radius cylindrical of InAs and MgO.

Aim of the Study

Our aim is to write this paper to study the surface properties of semiconducting compounds in magnetic field.

Review of Literature

Surface Plasmon Polaritons (SPP) has been an attractive and extensively studied topic in the scientific community for its various unique features. It has shown promising applications in many fields such as highly integrated optical circuits, high sensitive biological sensing, enhancing light matter interaction, and so on [1–7]. Although SPP modes can be designed by varying the metal structure, the frequency range and propagation loss still depends on the metal material. Dielectrics with large permittivity e1, such as Si or GaAs which are well used in some functional SPP devices [8-9], would lead to the decrease of surface Plasmon frequency and the cut off of SPP mode. In some cases, even though SPP mode is not cut off, the surrounding with large permittivity would result in extremely large propagation loss at certain optical frequency range. Meta-material at optical frequency can be regarded as a kind of man-made material with properties beyond natural materials[10].

Study of Filtering Properties

The dispersion relation for surface Plasma, Polaritons and Phonons including spatial dispersion relation is-

$$RX_1^{'}\left(ykR\right)\left(\frac{\varepsilon_\infty\left(k\omega\right)\Omega^2-\varepsilon_0\left(k\omega\right)\frac{\omega_t^2}{\omega_p^2}}{\Omega^2-\frac{\omega_t^2}{\omega_p^2}}\right)\left[\left\{\bar{\varepsilon}\left(kw\right)-\left(\frac{\varepsilon_\infty\left(k\omega\right)\Omega^2-\varepsilon_0\left(k\omega\right)0\frac{\omega_t^2}{\omega_p^2}}{\Omega^2-\frac{\omega_t^2}{\omega_p^2}}\right)\Omega^2/RZ(\partial kR/^{'}\right\}\right.$$

P: ISSN NO.: 2321-290X RNI : UPBIL/2013/55327 VOL-4* ISSUE-11* July- 2017
E: ISSN NO.: 2349-980X **Shrinkhla Ek Shodhparak Vaicharik Patrika**

$$\left(X(\gamma kR)\right)Y(\alpha kR)+\varepsilon_B(k\omega)\Omega^2\left(RX(\gamma kR)\right)'Z(\delta kR)\Big]$$

$$-1(1+1)X(\gamma kR)Y(\alpha kR)Z(\partial kR)\varepsilon_B(k\omega)\bar{\varepsilon}(k\omega)=0$$

(1)

Further study of the dispersion relation for surface plasmon, phonon, polariton, for non-spatially dispersion case, from eq. (1) by taking the limit γR→∞ and ξ→0, then eq. becomes in a new form-

$$\Omega^2\left(\frac{\omega_p}{\omega_t}\right)^2\varepsilon_\infty-\left[\varepsilon_0+\left\{\bar{\varepsilon}-(1+\varepsilon_\infty)k^2\right\}\left(\frac{\omega_p}{\omega_t}\right)^2\right]\Omega^4$$

$$+\left[\left\{(1+\varepsilon_0)+\bar{\varepsilon}\left(\frac{\omega_p}{\omega_t}\right)^2\right\}k^2+\bar{\varepsilon}\right]\Omega^2-\bar{\varepsilon}k^2=0$$

(2)

Table 1- For in As ε=14.9, ε_∞=12.3, $\bar{\varepsilon}$=13.6, ω_t=4.1 x $10^{13}s^{-1}$,
ω_p=4.77 x $10^{13}s^{-1}$.

Then equation (2) become into a new form-

$16.65\Omega^2$-$(33.3-18k^2)\Omega^4$+$(34.3k^2+13.6)\Omega^2$-$13.6k^2=0$

(3)

The equation (3) gives three values of Ω_1, Ω_2 *and* Ω_3 for different values of K.

K	Ω1	Ω2	Ω3
10	0.76091	5.14337	10.6371
20	0.7599	5.15559	23.0963
30	0.7597	5.17533	45.5288
40	0.7596	5.18220	45.5288
50	0.7596	5.18511	56.8732

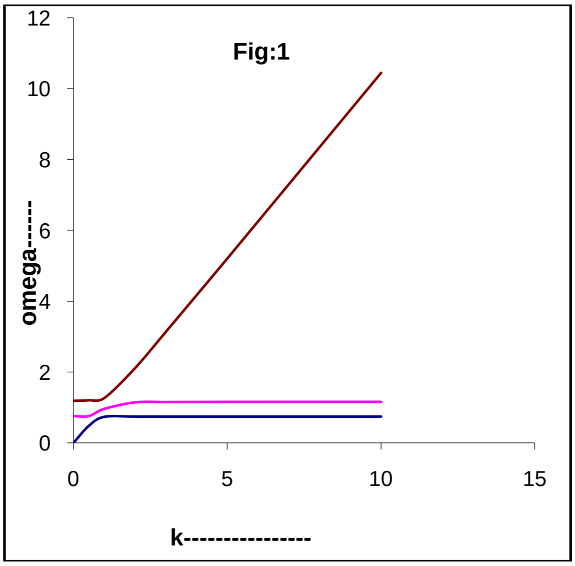

Table -2

The equation (2) can also be written as

$\omega = \omega/\omega_t$ and $\overline{k_1}=\frac{c_k}{\omega_t}$

then

$$\varepsilon_\infty\omega^6-\left[\bar{\varepsilon}\left(\frac{\omega_P}{\omega_t}\right)^2+\varepsilon_0+(1+\varepsilon_\infty)k_l^2\right]\omega^4+$$

$$\left[(1+\varepsilon_0)k_l^2+\bar{\varepsilon}\left(\frac{\omega_p}{\omega_t}\right)^2\right]\omega^2-\bar{\varepsilon}\left(\frac{\omega_P}{\omega_t}\right)^2k_l^2=0$$

(4)

Now putting the values, we get

$$12.3\omega^6-(14.9+13.3{k_l}^2)\omega^4$$
$$+(34.3{k_1}^2+18.4)\omega^2-18.4({k_1}^2)=0 \quad (5)$$

Then we get three roots of ω-

Sl. No	K	Ω1	Ω2	Ω3
1	0.0	0.000	0.756	1.190
2	0.5	0.487	0.760	1.205
3	1.0	0.742	0.960	1.268
4	2.0	0.749	1.143	2.111
5	3.0	0.749	1.153	3.136
6	4.0	0.749	1.155	4.170
7	5.0	0.749	1.157	5.208
8	10.0	0.749	1.158	10.450

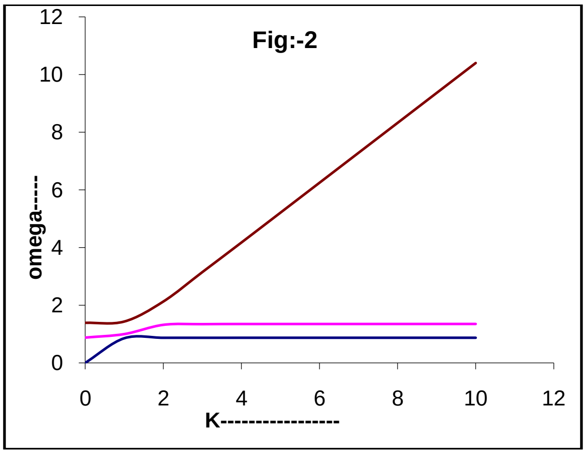

Table 3

The equation (2) can be also modified in terms of refractive index 'n'

$$n^2=\left[\frac{\Omega^2(12.3\Omega^2-(11)-13.6(\Omega^2-0.74))}{(\Omega^2-0.74)(\Omega^2-13.6)-\Omega^2(12.3\Omega^2-(11))}\right]$$

(6)

Sl. No.	Ω^2	m^2	ε(Ω)
1	0	1	-∞
2	0.1	1.008	-120
3	0.2	1.019	-52.18
4	0.3	1.036	-28.71
5	0.4	1.066	-16.11
6	0.5	1.166	-6.99
7	0.6	-0.65	-0.39
8	0.7	0.76	0.39
9	0.8	0.975	40.32

10	0.9	1.028	-36.33
11	1	1.07	-14.67
12	1.1	1.13	-8.6
13	1.2	1.23	-5.33
14	1.3	1.46	-3.15
15	1.4	2.81	-1.55
16	1.5	-0.408	-0.29
17	1.6	0.423	0.73
18	1.7	0.61	1.59
19	1.8	0.699	2.32
20	1.9	0.747	2.95
21	2	0.786	3.5
22	2.1	0.799	3.99

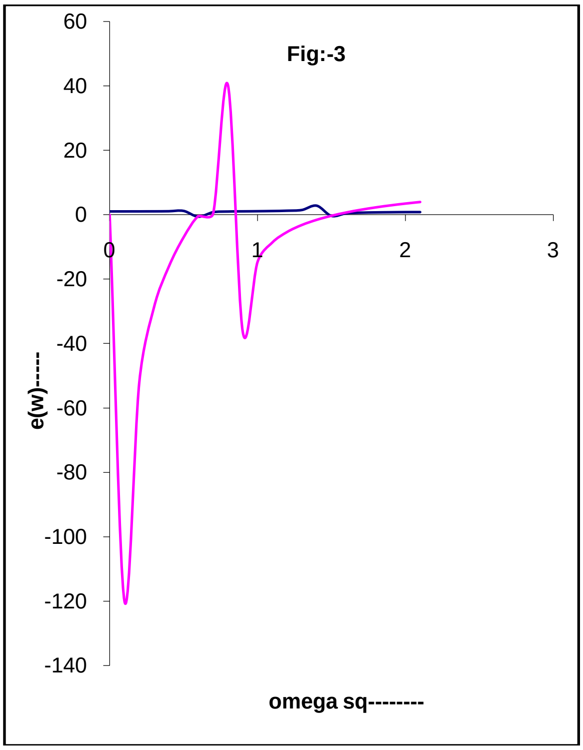

Conclusions

It is clear from fig (1) that the coupled surface plasmon and surface optical phonon modes lies between the two bounded non-radiative coupled modes. The lower coupled mode is non radiative for all values of wave vectors, the upper coupled modes crosses the light line for k = 0.75 and is thus radiative for k<0.75 and non-radiative for higher values of k. This implies that the corresponding values of frequency Ω are such that the dielectric function of the active medium no longer remains negative in this region but becomes positive which is the condition for existence of radiative surface modes.

Now we observe from the fig. (2) that the lower two modes are bound and non radiative whereas the upper mode lies above the pure photon modes, is radiative.

When, we observe the fig. (3) we find that there are two discontinuities at the two values of frequencies ($\Omega^2 = 0.56\ and\ 1.34$) i.e. (Ω=0.75 and Ω=1.16) in the plot of n^2 tends to ∞. These values of frequencies, for InAs polar semiconductor, as clear from fig. (3). At these points, the frequency values of the incident EM radiation match exactly with the coupled SP-SOP mode frequencies, leading to strong coupling which results in surface plasmon, phonon polariton modes. Thus at these points, there is a strong resonance between the incident EM wave and strong coupled SP-SOP excitation modes. Therefore at these values of frequency of the incident EM wave, no light is transmitted through the medium, the whole energy propagates as bound surface polariton wave along the interface. It is clear that the value of ε(Ω) is (-0.1), which is the condition of existence of bound, non-radiative surface mode.

The value of n^2 remains negative in the narrow range between $\Omega^2 = 0.56$ and 0.58, and again $\Omega^2 = 1.42$. thus for these two ranges of frequency of index of refraction of the medium, become imaginary this indicates that incident EM waves of these frequency range will be totally reflected. Thus n^2>1, values correspond to the non radiative. For n^2<1,ε(Ω) is positive. This occurs for the frequency range between $\Omega^2 = 0.58$ and 0.74 and then square of Ω> 1.42, thus for these values of frequency the condition for radiative Brewster surface mode is satisfied. The values of n^2 become zero at two points for $\Omega^2 = 0.58$ and for 1.42. Thus the surface wave can be transferred to the bulk of the medium. In other words, at these frequencies the condition for perfect transmission of incident EM wave is satisfied.

The incident radiation is not transmitted through the active medium for those ranges of frequencies for which the surface modes are bound and non-radiative. For those values of frequency for which the surface mode become radiative, the incident energy can be filtered or transmitted through the medium. It is clear that for Ω=0.76 and for 0.848 the medium become transparent to the incident radiation in this range. Above these frequency range between Ω=0.848 and Ω=1.119, the surface modes become non radiative so that the medium become opaque, for the incident EM radiation. For Ω>1.119 and higher values the surface again become transparent. Thus the surface of polar semiconductor acts as a high pass and band pass filter for incident EM waves.

The above discussion clearly indicates that during experimental study of polar semiconductor sphere by scattering and absorption of incident EM radiation, two absorption peaks will be obtained in the case of small spheres at the two coupled modes frequencies which lies in the region 0<$\frac{\omega}{\omega_t}$<$\frac{\omega_-}{\omega_+}$ and 1<$\frac{\omega}{\omega_t} < \frac{\omega_+}{\omega_t}$, where $\frac{\omega_-}{\omega_t}$ and $\frac{\omega_+}{\omega_t}$ are the roots of zeroes at dielectric function of polar semiconductor given by –

$$\varepsilon(\omega) = \frac{\varepsilon_\infty \omega^2 - \varepsilon_0 \omega_t^2}{\omega^2 - \omega_t^2} - \bar{\varepsilon}\frac{{\omega_p}^2}{\omega^2} \qquad (7)$$

In the frequency range defined above where the coupled SP-SOP modes exist, the dielectric function has a negative value. For larger sphere, tends to plane interface value, a third peak due to the bulk mode also appears in the absorption spectrum in the region $\frac{\omega_-}{\omega_+} < \frac{\omega}{\omega_t} < 1$ in between the two peaks due to the coupled surface modes.

Table .4 for graph between Ω and K of MgO.

Sl.no	K	Ω1	Ω2	Ω3
1	0.0	0.000	0.880	1.391
2	1.0	0.855	1.000	1.435
3	2.0	0.871	1.317	2.128
4	3.0	0.871	1.340	3.150
5	4.0	0.872	1.345	4.175
6	5.0	0.872	1.345	5.212
7	10.0	0.872	1.347	10.405

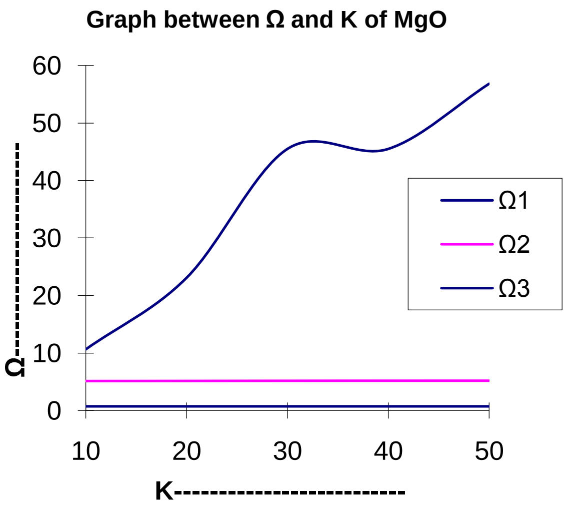

Fig.4

Results

As the value of k is increased the lower coupled mode is non radiative for all values of wave vectors, the upper coupled modes crosses the light line for variable k. Sharp change is observed for K>30, and further the gradual increase fixed a positive value.

References

1. *S.A. Maier, H.A. Atwater, Plasmonics: localization and guiding of electromagnetic energy in metal/dielectric structures. J. Appl. Phys. 98, 011101 (2005).*
2. *W. Yan, L.F. Shen, L.X. Ran, J.A. Kong, Surface modes at the interfaces between isotropic media and indefinite media. J. Opt. Soc. Am. A: 24(2), 530–535 (2007).*
3. *D. Zhang, Q. Zhang, Y. Lu, Y. Yao, S. Li, J. Jiang, G.L. Liu, Q. Liu, Peptide functionalized nanoplasmonic sensor for explosive detection. Nano-Micro Lett.8(1), 36–43 (2016).*
4. *S. Zeng, K.V. Sreekanth, J. Shang, T. Yu, C. Chen et al., Graphene–gold metasurface architectures for ultrasensitive plasmonicbiose-nsing. Adv. Mater. 27(40), 6163–6169 (2015).*
5. *O. Takayama, D. Artigas, L. Torner, Lossless directional guiding of light in dielectric nanosheets using Dyakonov surface waves. Nat. Nanotechnol. 9(6), 419–424 (2014).*
6. *M. Sun, T. Sun, Y. Liu, L. Zhu, F. Liu, Y. Huang, C.C. Hasnain, Integrated Plasmonic Refractive Index Sensor Based on Grating/ Metal Film Resonant Structure, Proc. SPIE 9757, High Contrast Metastructures V, (March 15, 2016): SPIE, 97570Q.*
7. *H.T.M. Baltar, K. Drozdowicz-Tomsia, E.M. Goldys, Plasmonics Principles and Applications (K. Y. Kim, Eds), InTech, Rijeka, pp. 136–155 (2012)*
8. *J.T. Kim, J.J. Ju, S. Park, M. Kim, S.K. Park, M.-H. Lee, Chip-tochip optical interconnect using gold long-range surface plasmonpolariton waveguides. Opt. Express 16(17), 13133–13138 (2008).*
9. *Y. Li, H. Zhang, T. Mei, N. Zhu, D.H. Zhang, J. Teng, Effect of dielectric cladding on active plasmonic device based on InGaAsP multiple quantum wells. Opt. Express 22(21), 25599–25607 (2014).*
10. *P. Shekhar, J. Atkinson, Z. Jacob, Hyperbolic metamaterials: fundamentals and applications. Nano Convergence 1(1), 14 (2014).*